Proposed Detection of Time Reversal Symmetry in Topological Surface States

Degang Zhang[1,2,3] and C. S. Ting[3]

[1]College of Physics and Electronic Engineering, Sichuan Normal University, Chengdu 610101, China
[2]Institute of Solid State Physics, Sichuan Normal University, Chengdu 610101, China
[3]Texas Center for Superconductivity and Department of Physics, University of Houston, Houston, TX 77204, USA

By employing T-matrix approach, we investigate a nonmagnetic impurity located on the surface of three-dimensional topological insulators, where the time reversal symmetry is preserved. It is shown that the images of the local density of states (LDOS) around the single impurity have the dip-hump structures with six-fold symmetry at different bias voltages. The peaks are produced by quasiparticle interference while the local minima at the backscattering wave vectors are due to the absence of backscatterings. With increasing the bias voltage, the peaks and dips move forward to the location of the impurity. These dips at the backscattering wave vectors in the LDOS spectra can be regarded as a signature of the time reversal symmetry in the topological surface states, which could be observed by scanning tunneling microscopy.

PACS numbers: 73.20.-r, 72.10.-d, 72.25.-b

In recent years much attention has been focused on the topological surface states due to their potential applications in quantum computing or spintronics [1,2]. The Dirac-cone-like electronic states, existing on the surface of three-dimensional bulk insulating materials, have been observed in $Bi_{1-x}Sb_x$ [3], Bi_2Sb_3 [4], Sb_2Te_3 [5], Bi_2Te_3 [5,6], $TlBiSe_2$ and $TlBiTe_2$ [7], by angle-resolved photoemission spectroscopy (ARPES). The surface energy band structure was determined by employing $k\cdot p$ theory [8], where an unconventional hexagonal warping term plays a crucial role in fitting the ARPES data [3-7] and in explaining the scanning tunneling microscopy (STM) experiments [9-13].

It is known that the novel topological surface states possess time reversal symmetry (TRS), which leads to the absence of backscatterings. Such a symmetry induces unusual electron transport properties on the surface of topological insulators [9-13]. Therefore, it is interesting to explore the TRS in order to understand thoroughly the physical properties of topological insulators. In this work, we give a proposal for experimental detection of the TRS in the topological surface states. We note that the oscillations of local density of states (LDOS) induced by a step or line defect can be explained satisfically by quasiparticle interference (QPI) and seem not to exhibit the existence of the TRS due to no direct evidence showing the absence of backscatterings. [9-13]. Here we employ a nonmagnetic impurity located on the surface of topological insulators in order to detect this symmetry. Such a single impurity has also been used to judge the superconducting order parameter symmetry in the cuprates and the FeAs-based superconductors [14-16]. In Refs. [17,18], the Fourier transformation of the LDOS induced by a nonmagnetic impurity was calculated. However, the oscillations of the LDOS with the hexagonal warping term and the role of the TRS in real space are never discussed previously.

The momentum space Hamiltonian describing the surface states of three-dimensional topological insulators reads [8]

$$H_0=\sum_{\mathbf{k}} C^{\dagger}_{\mathbf{k}}[(\frac{k^2}{2m^*}-\mu)I+v(k_x\sigma_y-k_y\sigma_x)+\lambda\phi_{\mathbf{k}}\sigma_z]C_{\mathbf{k}}, \quad (1)$$

where $C^{\dagger}_{\mathbf{k}}=(c^{\dagger}_{\mathbf{k}\uparrow},c^{\dagger}_{\mathbf{k}\downarrow})$, I and $\sigma_i (i=x,y,z)$ are the 2×2 unit matrix and the Pauli matrices, respectively, m^* is the effective mass of electrons, which is usually very large for the topological insulators, μ is the chemical potential to be determined by doping [10], v is the strength of the Rashba spin-orbit coupling, the last term is the so called hexagonal warping term, and $\phi_{\mathbf{k}}\equiv k_x(k_x^2-3k_y^2)$. Taking the linear transformations $c_{\mathbf{k}\uparrow}=\frac{1}{\sqrt{2}}\sum_{s=0,1}\alpha_{\mathbf{k}s}a_{\mathbf{k}s}\psi_{\mathbf{k}s}$ and $c_{\mathbf{k}\downarrow}=\frac{1}{\sqrt{2}}\sum_{s=0,1}\beta_{\mathbf{k}s}a_{\mathbf{k}s+1}\psi_{\mathbf{k}s}$ with $\alpha_{\mathbf{k}s}=1-s+s(ik_x+k_y)k^{-1}$, $\beta_{\mathbf{k}s}=s+(1-s)(ik_x-k_y)k^{-1}$, $a_{\mathbf{k}s}=cos\frac{\theta_{\mathbf{k}}}{2}+(-1)^s sin\frac{\theta_{\mathbf{k}}}{2}$, $\theta_{\mathbf{k}}=arctan\frac{\lambda\phi_{\mathbf{k}}}{vk}$, and $k=\sqrt{k_x^2+k_y^2}$, we have $H_0=\sum_{\mathbf{k}s}E_{\mathbf{k}s}\psi^{\dagger}_{\mathbf{k}s}\psi_{\mathbf{k}s}$ with the eigenenergies $E_{\mathbf{k}s}=\frac{k^2}{2m^*}+(-1)^s\sqrt{\lambda^2\phi_{\mathbf{k}}^2+v^2k^2}-\mu$.

Now we investigate a singe impurity located at the origin $\mathbf{r}=(0,0)$ on the surface of three-dimensional topological insulators. Without loss of generality, such an impurity can be described by the Hamiltonian $H_{\rm imp}=U\sum_{\sigma}c^{\dagger}_{\mathbf{0}\sigma}c_{\mathbf{0}\sigma}+V_{\rm m}(c^{\dagger}_{\mathbf{0}\uparrow}c_{\mathbf{0}\uparrow}-c^{\dagger}_{\mathbf{0}\downarrow}c_{\mathbf{0}\downarrow})$. Here U and $V_{\rm m}$ are the nonmagnetic and magnetic parts of the impurity strength, respectively. We solve the total Hamiltonian $H=H_0+H_{\rm imp}$ by employing T-matrix approach [15,16] and finally obtain the analytical expression of the LDOS around the impurity

$$\rho(\mathbf{r},\omega)\equiv\sum_{\mathbf{k}\mathbf{k}'ss'}\rho^{\mathbf{k}'s'}_{\mathbf{k}s}(\mathbf{r},\omega)$$

$$=-\frac{1}{2N\pi}{\rm Im}\sum_{\mathbf{k}\mathbf{k}'ss'}e^{i(\mathbf{k}-\mathbf{k}')\cdot\mathbf{r}}(\alpha_{\mathbf{k}s}\alpha^*_{\mathbf{k}'s'}a_{\mathbf{k}s}a_{\mathbf{k}'s'}$$

$$+\beta_{\mathbf{k}s}\beta^*_{\mathbf{k}'s'}a_{\mathbf{k}s+1}a_{\mathbf{k}'s'+1})G^{\mathbf{k}'s'}_{\mathbf{k}s}(i\omega_n)|_{i\omega_n\to\omega+i0^+}, \quad (2)$$

where N is the number of lattices, $\rho^{\mathbf{k}'s'}_{\mathbf{k}s}(\mathbf{r},\omega)$ represents the LDOS contributed by the scattering process $(\mathbf{k}s)\to(\mathbf{k}'s')$, and the Green's functions $G^{\mathbf{k}'s'}_{\mathbf{k}s}(i\omega_n)=G^0_{\mathbf{k}s}(i\omega_n)\delta_{\mathbf{k}\mathbf{k}'}\delta_{ss'}+G^0_{\mathbf{k}s}(i\omega_n)\mathcal{T}^{\mathbf{k}'s'}_{\mathbf{k}s}(i\omega_n)G^0_{\mathbf{k}'s'}(i\omega_n)$ with the bare Green's functions $G^0_{\mathbf{k}s}(i\omega_n)=(i\omega_n-E_{\mathbf{k}s})^{-1}$ and the T matrix

$$\mathcal{T}^{\mathbf{k}'s'}_{\mathbf{k}s}(i\omega_n)=\frac{U+V_m}{2N}\frac{\alpha^*_{\mathbf{k}s}a_{\mathbf{k}s}\alpha_{\mathbf{k}'s'}a_{\mathbf{k}'s'}}{[1-(U+V_m)A(i\omega_n)]}$$

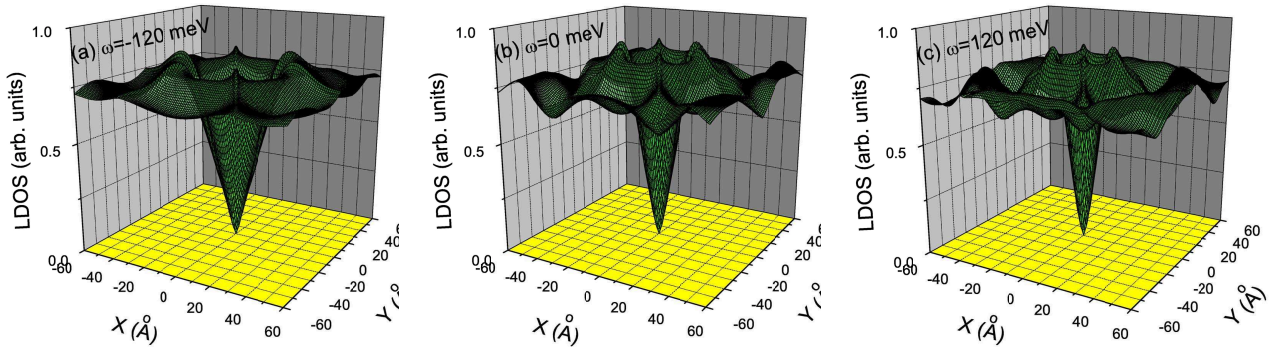

FIG. 1: (Color online) The stereographs of the LDOS $\rho(\mathbf{r},\omega)$ around a unitary impurity, i.e. $U\to\infty$, at different bias voltages.

$$+\frac{U-V_m}{2N}\frac{\beta^*_{\mathbf{k}s}a_{\mathbf{k}s+1}\beta_{\mathbf{k}'s'}a_{\mathbf{k}'s'+1}}{[1-(U-V_m)A(i\omega_n)]}. \quad (3)$$

Here, $A(i\omega_n)=\frac{1}{2N}\sum_{\mathbf{k}s}G^0_{\mathbf{k}s}(i\omega_n)$. When $V_m=0$, we have $\mathcal{T}^{-\mathbf{k}s}_{\mathbf{k}s}(i\omega_n)\equiv 0$. This means that there are no backscatterings at each constant-energy contour $\omega=E_{\mathbf{k}s}$ [17,18]. In other words, the surface states with opposite momentum and the same s are still orthogonal and do not mix after being scattered by a pure nonmagnetic impurity. So there is no interference between the two surface states connected by a backscattering wave vector. From Eq. (2), we can also see that the backscattering processes have no contribution to the LDOS, i.e. $\rho^{-\mathbf{k}s}_{\mathbf{k}s}(\mathbf{r},\omega)\equiv 0$. Therefore, the LDOS induced by a nonmagnetic impurity should has the local minima at the backscattering wave vectors. Such the dips are produced by the absence of backscatterings rather than the QPI, which could be used to detect the TRS in the topological surface states.

According to Eq. (2), we can calculate the LDOS around the single impurity, which is measured by STM experiments. In our calculations, we choose a 120×120Å^2 lattice with $N=1800\times1800$ and employ the physical parameters in Bi_2Sb_3, i.e. $\lambda=250.0$ eV·Å^3, $v=2.55$ eV·Å, and $\mu=0.334$ eV [8,10].

In Fig. 1, we present the stereographs of the LDOS induced by a unitary impurity ($U\to\infty$) at $\omega=-120,0,120$ (meV). Such the infinite potential has been realized by the Zn ions in the cuprates [14], which is also expected to exist on the surface of topological insulators. Obviously, $\rho(\mathbf{r},\omega)$ has a dip-hump structure with a six-fold symmetry at each bias voltage. When the bias voltage ω increases, these peaks and dips move forward to the location of the impurity. On the impurity site, we have $\rho(\mathbf{r},\omega)|_{\mathbf{r}=(0,0)}=0$.

In order to understand clearly the energy-dependent peaks and dips in the LDOS, we depict the constant-energy contours of the surface energy band at $\omega=-120,0,120$ (meV) in Fig. 2. There are six modulation wave vectors $\mathbf{q}_{K1}$, $\mathbf{q}_{K2}$, $\mathbf{q}_{KB}$, $\mathbf{q}_{M1}$, $\mathbf{q}_{M2}$, $\mathbf{q}_{MB}$, and their corresponding symmetric wave vectors induced by the QPI. $\mathbf{q}_{KB}$ and $\mathbf{q}_{MB}$ are the backscattering wave vectors connecting two opposite K points and two opposite M points, respectively. According to the symmetry of the constant-energy contours, we have $|\mathbf{q}_{K1}|=\frac{1}{2}|\mathbf{q}_{KB}|$, $|\mathbf{q}_{K2}|=\frac{\sqrt{3}}{2}|\mathbf{q}_{KB}|$, $|\mathbf{q}_{M1}|=\frac{1}{2}|\mathbf{q}_{MB}|$, and $|\mathbf{q}_{M2}|=\frac{\sqrt{3}}{2}|\mathbf{q}_{MB}|$. We also note that the wave vectors $\mathbf{q}_{K1}$, $\mathbf{q}_{KB}$, and $\mathbf{q}_{M2}$ ($\mathbf{q}_{M1}$, $\mathbf{q}_{MB}$, and $\mathbf{q}_{K2}$) are along the same modulation direction, i.e. $\mathbf{q}_{K1}//\mathbf{q}_{KB}//\mathbf{q}_{M2}$ ($\mathbf{q}_{M1}//\mathbf{q}_{MB}//\mathbf{q}_{K2}$). The angle between the two modulation directions is *integer* $\cdot\,60^\circ+30^\circ$. Due to the existence of a backscattering wave vector and two QPI wave vectors in the same direction, we shall observe below that the peaks and dips in the images of the LDOS seem not to locate exactly at these modulation wave vectors. When $\omega=-120$ meV, $|\mathbf{q}_{M2}|\approx|\mathbf{q}_{KB}|$. With increasing the energy, all the modulation wave vectors become longer, but the increasing length of each wave vector is different. Therefore, the competition among the wave vectors produces abundant energy-dependent structures in the LDOS. The oscillation periods corresponding to these wave vectors have the relations: $T_{K1}=\frac{2\pi}{|\mathbf{q}_{K1}|}=2T_{KB}$, $T_{K2}=\frac{2\pi}{|\mathbf{q}_{K2}|}=\frac{2}{\sqrt{3}}T_{KB}$, $T_{M1}=\frac{2\pi}{|\mathbf{q}_{M1}|}=2T_{MB}$, and $T_{M2}=\frac{2\pi}{|\mathbf{q}_{M2}|}=\frac{2}{\sqrt{3}}T_{MB}$.

Fig. 3 shows the images of the LDOS with a moderate nonmagnetic potential $U=5.0$ eV and $V_m=0$ eV at $\omega=-120,0,120$ (meV), where the TRS persists. When $\omega=-120$ meV, the LDOS $\rho(\mathbf{r},\omega)$ has the local minima at $r=T_{K2},T_{M2},T_{KB}$, and T_{MB}. Because $|T_{M2}|\approx|T_{KB}|$ and $|T_{K2}|\sim|T_{MB}|$, these dips are produced by both the QPI and the absence of backscatterings. With increasing the bias voltage, the local minima move forward to the origin and form a hexagonal sinkage around the impurity at $\omega=0$ meV. Obviously, $\rho(\mathbf{r},\omega)$ also has the peaks at $r=T_{K1}$ and T_{M1} while the dips show up at $2T_{M2}$ in Fig. 3(b). Because $T_{K1}=2T_{KB}$ and $T_{M1}=2T_{MB}$, the effect of the QPI on the LDOS is

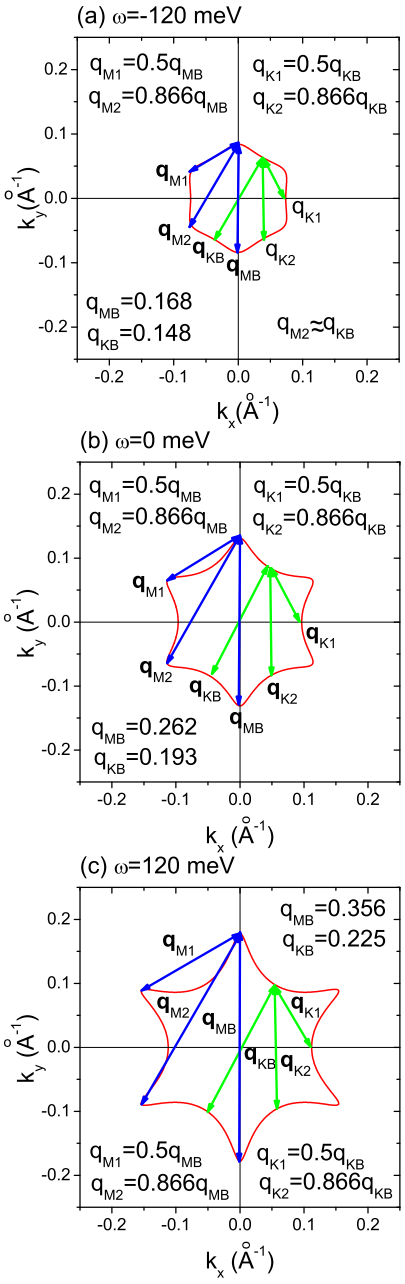

FIG. 2: (Color online) The constant-energy contours of the surface state band at different energies. The modulation wave vectors in the LDOS are shown.

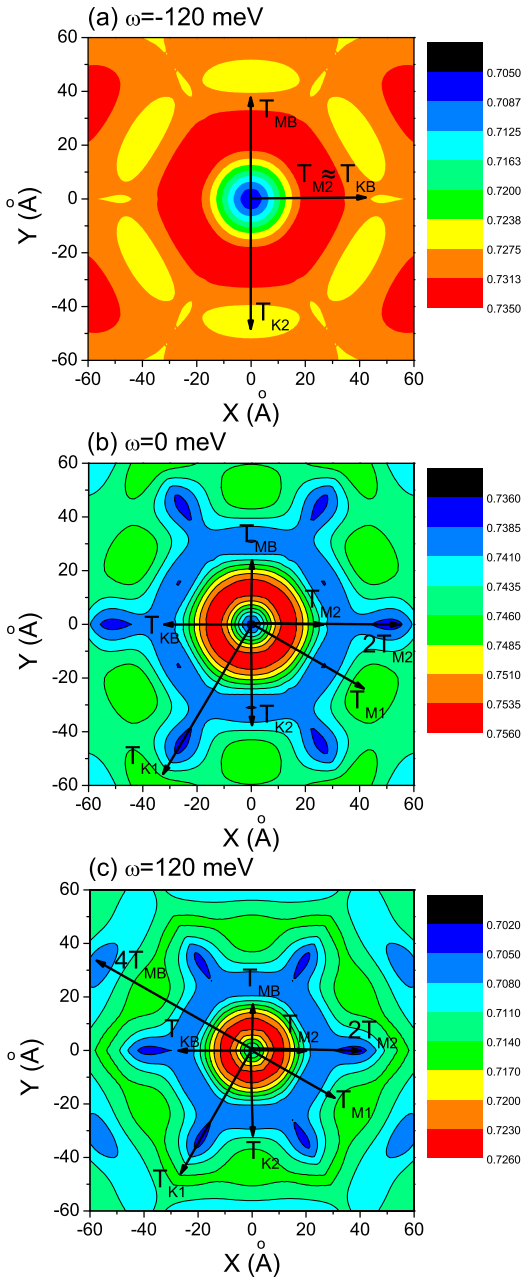

FIG. 3: (Color online) The images of the LDOS with the pure nonmagnetic potential $U = 5.0$ eV at different bias voltages.

stronger than that of the TRS near the impurity. However, when $\omega = 120$ meV, the LDOS possesses the local minima at $r = 4T_{MB} = 2T_{M1}$, shown in Fig. 3(c). This means that the effect of the TRS on the LDOS is dominant far from the impurity. Therefore, the Friedel oscillations induced by the QPI decay faster than those due to the TRS.

To further elucidate the origin of the dips at the backscattering wave vectors, we also calculate the LDOS produced by a magnetic potential $V_m = 10.0$ eV and $U = 0$ eV, where the TRS is broken. Therefore, the backscatterings are allowed. When $\omega = -120$ meV, the LDOS has higher peaks at $r = T_{M2}$, opposite with a pure nonmagnetic impurity, while there are also the dips at $r = T_{K2}$. However, $\rho(\mathbf{r}, \omega)$ has no obvious peaks or dips at $\mathbf{q}_{MB}$ and $\mathbf{q}_{KB}$. So the QPI can be neglected at the backscattering wave vectors. Therefore, the dips at the backscattering wave vectors are indeed produced by the TRS in the presence of a nonmagnetic impurity. When the energy increases, the peaks and the dips also move forward to the magnetic impurity, similar to a nonmagnetic potential. In Fig. 4(b) and 4(c), the LDOS has the local minima at $r = T_{K1}$ and T_{M1}, contrary to a nonmagnetic impurity.

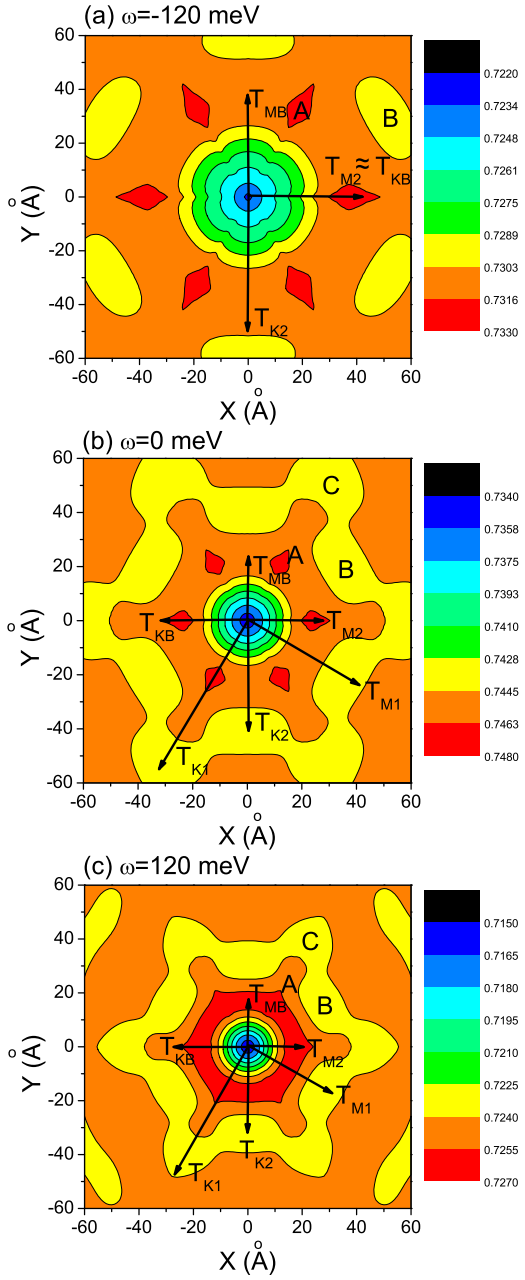

FIG. 4: (Color online) The images of the LDOS with the pure magnetic potential V_m = 10.0 eV at different bias voltages.

In summary, we have proposed a method to detect the TRS in topological surface states. Due to this symmetry, the topological surface states with opposite momentum and the same s are incoherent and contribute zero to the LDOS. Therefore, the dips at the backscattering wave vectors in the LDOS induced by a nonmagnetic impurity can be regarded a signature of the TRS. We note that in each modulation direction there is the competition between a backscattering wave vector and two QPI wave vectors, which leads to robust dip-hump features in the LDOS. Because the peaks induced by the QPI decay faster than the dips produced by the TRS, it is easy to observe the local minima at the backscattering wave vectors at higher bias voltages and several periods away from the nonmagnetic impurity by STM experiments.

This work was supported by the Sichuan Normal University, by the Texas Center for Superconductivity at the University of Houston, and by the Robert A. Welch Foundation under the Grant no. E-1411.

[1] Xiao-Liang Qi and Shou-Cheng Zhang, Phys. Today **63**, 33 (2010); Rev. Mod. Phys. **83**, 1057 (2011).
[2] M. Z. Hasan and C. L. Kane, Rev. Mod. Phys. **82**, 3045 (2010).
[3] D. Hsieh, Y. Xia, L. Wray, D. Qian, A. Pal, J. H. Dil, F. Meier, J. Osterwalder, G. Bihlmayer, C. L. Kane, Y. S. Hor, R. J. Cava, M. Z. Hasan, Science **323**, 919 (2009).
[4] Y. Xia, D. Qian, D. Hsieh, L. Wray, A. Pal, H. Lin, A. Bansil, D. Grauer, Y. S. Hor, R. J. Cava, M. Z. Hasan, Nature Phys. **5**, 398 (2009).
[5] Haijun Zhang, Chao-Xing Liu, Xiao-Liang Qi, Xi Dai, Zhong Fang and Shou-Cheng Zhang, Nature Phys. **5**, 438 (2009).
[6] Y. L. Chen, J. G. Analytis, J.-H. Chu, Z. K. Liu, S.-K. Mo, X. L. Qi, H. J. Zhang, D. H. Lu, X. Dai, Z. Fang, S. C. Zhang, I. R. Fisher, Z. Hussain, and Z.-X. Shen, Science **325**, 178 (2009).
[7] Y. L. Chen, Z. K. Liu, J. G. Analytis, J.-H. Chu, H. J. Zhang, B. H. Yan, S.-K. Mo, R. G. Moore, D. H. Lu, I. R. Fisher, S. C. Zhang, Z. Hussain, and Z.-X. Shen, Phys. Rev. Lett. **105**, 266401 (2010).
[8] Liang Fu, Phys. Rev. Lett. **103**, 266801 (2009).
[9] Tong Zhang, Peng Cheng, Xi Chen, Jin-Feng Jia, Xucun Ma, Ke He, Lili Wang, Haijun Zhang, Xi Dai, Zhong Fang, Xincheng Xie, and Qi-Kun Xue, Phys. Rev. Lett. **103**, 266803 (2009).
[10] Z. Alpichshev, J. G. Analytis, J.-H. Chu, I. R. Fisher, Y. L. Chen, Z. X. Shen, A. Fang, and A. Kapitulnik, Phys. Rev. Lett. **104**, 016401 (2010).
[11] K. K. Gomes, Wonhee Ko, Warren Mar, Yulin Chen, Zhi-Xun Shen, Hari C. Manoharan, arXiv:0909.0921 (unpublished).
[12] J. Seo, Pedram Roushan, Haim Beidenkopf, Y. S. Hor, R. J. Cava, Ali Yazdani, Nature (London) **466**, 343 (2010).
[13] Degang Zhang and C. S. Ting, Phys. Rev. B **85**, 115434 (2012); Jin An and C. S. Ting, Phys. Rev. B **86**, 165313 (2012).
[14] S.H. Pan, E.W. Hudson, K.M. Lang, H. Eisaki, S. Uchida, and J.C. Davis, Nature (London) **403**, 746 (2000).
[15] A. V. Balatsky, I. Vekhter, and J.-X. Zhu, Rev. Mod. Phys. **78**, 373 (2006).
[16] Degang Zhang, Phys. Rev. Lett. **103**, 186402 (2009); *ibid* **104**, 089702 (2010).
[17] Xiaoting Zhou, Chen Fang, Wei-Feng Tsai, and Jiangping Hu, Phys. Rev. B **80**, 245317 (2009).
[18] Wei-Cheng Lee, Congjun Wu, Daniel P. Arovas, and Shou-Cheng Zhang, Phys. Rev. B **80**, 245439 (2009).